Asociación Argentina
de Mecánica Computacional

Mecánica Computacional Vol XXIX, págs. 2775-2784 (artículo completo)
Eduardo Dvorkin, Marcela Goldschmit, Mario Storti (Eds.)
Buenos Aires, Argentina, 15-18 Noviembre 2010

DILATATIONAL VISCOPLASTICITY OF CUBIC POLYCRYSTALS WITH INTERGRANULAR CAVITIES

Martín I. Idiart[a,b], Ricardo A. Lebensohn[c] and Pedro Ponte Castañeda[d]

[a] *Departamento de Aeronáutica, Facultad de Ingeniería, Universidad Nacional de La Plata, Calles 1 y 47, La Plata B1900TAG, Argentina, martin.idiart@ing.unlp.edu.ar*

[b] *Consejo Nacional de Investigaciones Científicas y Técnicas (CONICET), Avda. Rivadavia 1917, Cdad. de Buenos Aires C1033AAJ, Argentina.*

[c] *Materials Science and Technology Division, Los Alamos National Laboratory, MS G755, Los Alamos, NM 87545, USA.*

[d] *Department of Mechanical Engineering and Applied Mechanics, University of Pennsylvania, Philadelphia, PA 19104-6315, USA.*

Keywords: porosity, texture, viscoplasticity, homogenization

Abstract. Theoretical predictions are derived for the viscoplastic response of polycrystalline solids containing a *random* distribution of intergranular porosity. The predictions follow from a nonlinear homogenization method based on a 'generalized secant' linearization of the viscoplastic crystal response, as proposed by Liu & Ponte Castañeda (*J. Mech. Phys. Solids* 52:467-495, 2004). The influence of crystallographic texture and porosity on the instantaneous response is investigated in the case of non-hardening power-law crystals with face-centered cubic symmetry. It is found that crystallinity of the matrix material has a minor effect, even when crystals exhibit a low strain-rate sensitivity. Thus, the assumption of matrix isotropy implicit in all standard theories of dilatational viscoplasticity should be appropriate for this class of materials.

1 INTRODUCTION

The aim of this work is to provide constitutive models for the finite-deformation viscoplastic response of polycrystalline aggregates accounting for the dilatational effects associated with the presence of intergranular cavities. Such constitutive models are required for the numerical simulation of many engineering applications (e.g., dynamic loading of polycrystalline materials, forming aggregates with initial porosity), where the dilatational effects associated with the presence of cavities must be accounted for, and standard polycrystalline models for incompressible plasticity are not appropriate. They are also needed to account for texture effects on ductile failure of metals —and other polycrystalline solids— by void growth to coalescence, as observed under both quasi-static (Bache and Evans, 2001; Lebensohn *et al.*, 1996; Hales and Hafley, 1998) and dynamic (Gray *et al.*, 1999) loading conditions. In the presence of a compressible voided phase, the elementary Taylor and Sachs approximations for polycrystalline solids are known to give unphysical predictions; alternative approaches are thus required. A dilatational viscoplasticity theory for voided polycrystals is derived in this work by extending a nonlinear homogenization method initially proposed by Liu and Ponte Castañeda (2004) for fully dense polycrystals. The resulting models are general enough to account for $i)$ morphological and crystallographic texture of the polycrystalline matrix, $ii)$ porosity, and $iii)$ average pore shape and orientation, as well as their deformation-induced evolution under arbitrary loading conditions. At the same time, the models should be simple enough to be implemented in dynamic finite-element codes. In this first study we will restrict attention to cubic polycrystals.

Voided polycrystals are idealized here as random aggregates of perfectly bonded single crystals —i.e., grains— and cavities. Individual grains and cavities are assumed to be of a similar size, much smaller than the specimen size and the scale of variation of the applied loads. Furthermore, aggregates are assumed to be statistically uniform and ergodic. Their viscoplastic behavior is most conveniently studied by adopting an Eulerian description of motion. At a generic stage of deformation, grains are assumed to individually deform by multi-glide along K slip systems. Cavities, on the other hand, cannot sustain stress. The effects of grain elasticity and possible twinning are neglected in this work, for simplicity. Let the grain orientations in the current configuration take on a set of N discrete values, characterized by rotation tensors $\mathbf{Q}^{(r)}$ ($r = 1, ..., N$). All grains with a given orientation $\mathbf{Q}^{(r)}$ are collectively referred to as 'phase' r, while all cavities are collectively referred to as 'phase' 0. The local viscoplastic response of the aggregate can then be described by a stress potential u, such that the Eulerian strain-rate tensor $\boldsymbol{D}$ and the stress tensor $\boldsymbol{\sigma}$ are related by

$$\boldsymbol{D} = \frac{\partial u}{\partial \boldsymbol{\sigma}}(\mathbf{x}, \boldsymbol{\sigma}), \quad u(\mathbf{x}, \boldsymbol{\sigma}) = \sum_{r=0}^{N} \chi^{(r)}(\mathbf{x}) u^{(r)}(\boldsymbol{\sigma}). \tag{1}$$

In this expression, the functions $\chi^{(r)}(\mathbf{x})$ are random variables that take the value 1 if the position vector $\mathbf{x}$ is in the domain of phase r and 0 otherwise, $u^{(0)}$ is the stress potential for the voided phase, which takes the value 0 if $\boldsymbol{\sigma} = \mathbf{0}$ and infinity otherwise, and $u^{(1)}, ..., u^{(N)}$ are the stress potentials characterizing grains with orientation $\mathbf{Q}^{(1)}, ..., \mathbf{Q}^{(N)}$, given by

$$u^{(r)}(\boldsymbol{\sigma}) = \sum_{k=1}^{K} \phi_{(k)}^{(r)} \left(\tau_{(k)}^{(r)} \right). \tag{2}$$

The convex functions $\phi_{(k)}^{(r)}$ ($k = 1, ..., K$) characterize the response of the K slip systems in a

crystal with orientation $\mathbf{Q}^{(r)}$, and depend on the resolved shear (or Schmid) stresses

$$\tau_{(k)}^{(r)} = \boldsymbol{\sigma} \cdot \boldsymbol{\mu}_{(k)}^{(r)}, \quad \text{where} \quad \boldsymbol{\mu}_{(k)}^{(r)} = \frac{1}{2}\left(\mathbf{n}_{(k)}^{(r)} \otimes \mathbf{m}_{(k)}^{(r)} + \mathbf{m}_{(k)}^{(r)} \otimes \mathbf{n}_{(k)}^{(r)}\right). \tag{3}$$

Here, the $\boldsymbol{\mu}_{(k)}^{(r)}$ are second-order tensors with $\mathbf{n}_{(k)}^{(r)}$ and $\mathbf{m}_{(k)}^{(r)}$ denoting the unit vectors normal to the slip plane and along the slip direction of the kth system, respectively, for a crystal with orientation $\mathbf{Q}^{(r)}$. Note that the Schmid tensors $\boldsymbol{\mu}_{(k)}^{(r)}$ are related to corresponding tensors $\boldsymbol{\mu}_{(k)}$ for a 'reference' crystal via $\boldsymbol{\mu}_{(k)}^{(r)} = \mathbf{Q}^{(r)^T}\boldsymbol{\mu}_{(k)}\mathbf{Q}^{(r)}$.

Due to the microstructural inhomogeneity, the local fields $\boldsymbol{D}(\mathbf{x})$ and $\boldsymbol{\sigma}(\mathbf{x})$ exhibit strong spatial variations within the aggregate. The effective viscoplastic behavior of the aggregate is obtained by homogenizing the local viscoplasticity problem. Let $\langle\cdot\rangle$ and $\langle\cdot\rangle^{(r)}$ denote volume averages over the aggregate and over each phase $^{(r)}$, respectively. The effective response can be formally written as (e.g., Ponte Castañeda and Suquet, 1998)

$$\overline{\boldsymbol{D}} = \frac{\partial \widetilde{u}}{\partial \overline{\boldsymbol{\sigma}}}(\overline{\boldsymbol{\sigma}}), \quad \widetilde{u}(\overline{\boldsymbol{\sigma}}) = \min_{\boldsymbol{\sigma}\in\mathcal{S}(\overline{\boldsymbol{\sigma}})} \langle u(\mathbf{x},\boldsymbol{\sigma})\rangle = (1-f)\min_{\boldsymbol{\sigma}\in\mathcal{S}^*(\overline{\boldsymbol{\sigma}})} \sum_{r=1}^{N} c_g^{(r)} \langle u^{(r)}(\boldsymbol{\sigma})\rangle^{(r)}, \tag{4}$$

where $\overline{\boldsymbol{\sigma}} = \langle\boldsymbol{\sigma}\rangle$ and $\overline{\boldsymbol{D}} = \langle\boldsymbol{D}\rangle$ are the average stress and strain rate over the aggregate, and $\widetilde{u}$ is the *effective stress potential*, f denotes the volume fraction of cavities –or porosity– and $c_g^{(r)}$ represents the volume fraction of the crystalline phase r within the matrix phase. Also, $\mathcal{S}(\overline{\boldsymbol{\sigma}})$ denotes the set of statically admissible stress fields with prescribed average $\overline{\boldsymbol{\sigma}}$, while $\mathcal{S}^* \subset \mathcal{S}$ denotes the subset of stress fields with zero traction vector on the surface of the cavities. Carrying out the minimization in (4) is in general a formidable task, since it requires the solution to sets of nonlinear partial differential equations with randomly oscillatory coefficients. In this work we generate approximate *estimates* for the effective potential by means of a variational 'linear-comparison' method.

2 NONLINEAR HOMOGENIZATION ESTIMATES

Following Liu and Ponte Castañeda (2004), the approach proposed in this work makes use of a 'linear-comparison polycrystal' (LCP) which consists of a polycrystal with the same microstructure as the nonlinear polycrystal but whose single-crystal response is identified with a certain linearization of the corresponding nonlinear response. Then, any of the available models for linear polycrystals can be used to estimate the effective potential of the linear-comparison polycrystal, which in turn can be used to estimate the effective potential of the nonlinear polycrystal.

The linearized crystalline phases are characterized by quadratic potentials of the form

$$u_L^{(r)}(\boldsymbol{\sigma}) = \frac{1}{2}\boldsymbol{\sigma}\cdot\mathbf{M}^{(r)}\boldsymbol{\sigma} + \mathbf{e}^{(r)}\cdot\boldsymbol{\sigma}, \tag{5}$$

where

$$\mathbf{M}^{(r)} = \sum_{k=1}^{K} \alpha_{(k)}^{(r)} \boldsymbol{\mu}_{(k)}^{(r)} \otimes \boldsymbol{\mu}_{(k)}^{(r)} \quad \text{and} \quad \mathbf{e}^{(r)} = \sum_{k=1}^{K} e_{(k)}^{(r)} \boldsymbol{\mu}_{(k)}^{(r)} \quad (r = 1, ..., N) \tag{6}$$

define the viscous-compliance and 'residual' strain-rate tensors at the grain level in terms of the corresponding slip-level quantities $\alpha_{(k)}^{(r)}$ and $e_{(k)}^{(r)}$, respectively. For the voided phase, in turn,

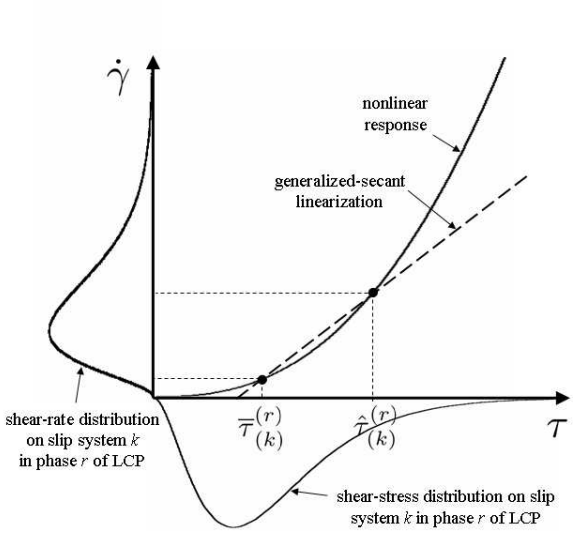

Figure 1: 'Generalized-secant' linearization scheme.

$(\mathbf{M}^{(0)})^{-1} = \mathbf{0}$ and $\mathbf{e}^{(0)} = \mathbf{0}$. Now, generalizing the theory of Liu and Ponte Castañeda (2004) to account for the additional vacuous phase, we approximate the local potentials $u^{(r)}$ of the nonlinear polycrystal in terms of the local potentials $u_L^{(r)}$ and a suitable measure of the error, to obtain the following approximation for the effective potential of the nonlinear polycrystal:

$$\widetilde{u}(\overline{\boldsymbol{\sigma}}) = (1-f)\sum_{r=1}^{N}\sum_{k=1}^{K} c_g^{(r)}\left[\phi_{(k)}^{(r)}(\hat{\tau}_{(k)}^{(r)}) - \phi_{(k)}^{(r)\prime}(\overline{\tau}_{(k)}^{(r)})(\hat{\tau}_{(k)}^{(r)} - \overline{\tau}_{(k)}^{(r)})\right], \tag{7}$$

where the variables $\hat{\tau}_{(k)}^{(r)}$ and $\overline{\tau}_{(k)}^{(r)}$ depend on the averages and fluctuations of the resolved shear stresses $\boldsymbol{\sigma}\cdot\boldsymbol{\mu}_{(k)}^{(r)}$ in the linear-comparison polycrystal subjected to the same macroscopic stress $\overline{\boldsymbol{\sigma}}$ as the nonlinear material. They are such that:

$$\overline{\tau}_{(k)}^{(r)} = \left\langle \boldsymbol{\sigma}\cdot\boldsymbol{\mu}_{(k)}^{(r)}\right\rangle^{(r)} = \overline{\boldsymbol{\sigma}}^{(r)}\cdot\boldsymbol{\mu}_{(k)}^{(r)} \tag{8}$$

and

$$(\hat{\tau}_{(k)}^{(r)} - \overline{\tau}_{(k)}^{(r)})^2 = \left\langle \left(\boldsymbol{\sigma}\cdot\boldsymbol{\mu}_{(k)}^{(r)} - \overline{\tau}_{(k)}^{(r)}\right)^2\right\rangle^{(r)} = \boldsymbol{\mu}_{(k)}^{(r)}\cdot\mathbf{C}_{\boldsymbol{\sigma}}^{(r)}\boldsymbol{\mu}_{(k)}^{(r)}, \tag{9}$$

where

$$\overline{\boldsymbol{\sigma}}^{(r)} = \langle\boldsymbol{\sigma}\rangle^{(r)} \quad \text{and} \quad \mathbf{C}_{\boldsymbol{\sigma}}^{(r)} = \left\langle(\boldsymbol{\sigma}-\overline{\boldsymbol{\sigma}}^{(r)})\otimes(\boldsymbol{\sigma}-\overline{\boldsymbol{\sigma}}^{(r)})\right\rangle^{(r)} = \langle\boldsymbol{\sigma}\otimes\boldsymbol{\sigma}\rangle^{(r)} - \overline{\boldsymbol{\sigma}}^{(r)}\otimes\overline{\boldsymbol{\sigma}}^{(r)}. \tag{10}$$

The quantities $\hat{\tau}_{(k)}^{(r)} - \overline{\tau}_{(k)}^{(r)}$ in (9) are taken to have the same sign as the $\overline{\tau}_{(k)}^{(r)}$.

The tensors (10) are given in terms of the local properties $\mathbf{M}^{(r)}$ and $\mathbf{e}^{(r)}$ according to the linear theory utilized. A particularly accurate and easy-to-use theory is the so-called *self-consistent* model (see Lebensohn et al., 2004). This linear model was originally proposed —in the mathematically analogous context of linear elasticity— as an ad-hoc model by Hershey (1954) and Köner (1958), and was later derived more rigorously and endowed with a clear statistical interpretation by Willis (1977). Self-consistent estimates for the tensors $\overline{\boldsymbol{\sigma}}^{(r)}$ and $\mathbf{C}_{\boldsymbol{\sigma}}^{(r)}$ can be found, for instance, in Liu and Ponte Castañeda (2004) —see Section 3.3 in that Reference.

In turn, the properties of the linear-comparison polycrystal must be specified such that the variables $e_{(k)}^{(r)}$ and $\alpha_{(k)}^{(r)}$ in relations (6) satisfy the relations

$$e_{(k)}^{(r)} = \phi_{(k)}^{(r)\prime}(\overline{\tau}_{(k)}^{(r)}) - \alpha_{(k)}^{(r)}\overline{\tau}_{(k)}^{(r)} \tag{11}$$

and

$$\phi_{(k)}^{(r)\prime}(\hat{\tau}_{(k)}^{(r)}) - \phi_{(k)}^{(r)\prime}(\overline{\tau}_{(k)}^{(r)}) = \alpha_{(k)}^{(r)}(\hat{\tau}_{(k)}^{(r)} - \overline{\tau}_{(k)}^{(r)}). \tag{12}$$

Note that relation (12) identifies the viscous slip compliances $\alpha_{(k)}^{(r)}$ of the linear-comparison polycrystal with a 'generalized-secant' approximation of the nonlinear constitutive relation for the corresponding slips systems in the viscoplastic polycrystal, taking into account both the average and fluctuation of the stress for the given grain orientation —as determined by the linear-comparison approximation, see Figure 1. Expressions (8)-(12) together with (10) constitute a system of nonlinear *algebraic* equations for the variables $\hat{\tau}_{(k)}^{(r)}$, $\overline{\tau}_{(k)}^{(r)}$ and $\alpha_{(k)}^{(r)}$, which must be solved numerically, in general. In this work, the equations are solved by means of the 'VPSC' FORTRAN code developed by Lebensohn and coworkers, suitably modified to account for the presence of a compressible voided phase. Details on the algorithm can be found in Tomé and Lebensohn (2007).

3 PREDICTIONS FOR CUBIC POWER-LAW POLYCRYSTALS

The 'generalized-secant' method presented above is used here to study the influence of crystallinity, texture and porosity on the instantaneous response of a special —but representative— class of cubic polycrystalline solids. Of particular interest in this study is to assess the simplifying assumption made in standard theories of dilatational viscoplasticity (e.g., Gurson, 1977) that the matrix material surrounding the cavities is isotropic. For this reason, attention is restricted to polycrystalline solids with *isotropic* microstructural statistics, that is, with 'equiaxed' grains and isotropically distributed porosity.

Crystals are assumed to exhibit face-centered cubic (fcc) symmetry and to deform plastically through slip on a set of four slip planes of the type $\{111\}$ along three slip directions (per plane) of type $\langle 110\rangle$, which, together, constitute a set of twelve slip systems with suitably defined Schmid tensors $\boldsymbol{\mu}_{(k)}^{(r)}$. Of these, five are linearly independent, allowing arbitrary plastic deformation for the grains (see Groves and Kelly, 1953). The viscous flow is characterized by potentials of the common power-law form

$$\phi_{(k)}(\tau) = \frac{\tau_0\dot{\gamma}_0}{n+1}\left|\frac{\tau}{\tau_0}\right|^{n+1} \tag{13}$$

for *all* grains. Here, $m = 1/n$ ($0 \leq m \leq 1$) is the strain-rate sensitivity, $\dot{\gamma}_0$ is a reference strain rate, and $\tau_0 > 0$ is the flow stress of the slip system in the 'reference' crystal. For simplicity, all systems are assumed to be nonhardening. This class of slip potentials is particularly appropriate for investigating the effect nonlinearity and grain anisotropy in a wide range of material behaviors. In particular, the limiting cases $m = 1$ and $m = 0$ correspond to linearly viscous and rigid-ideally plastic behaviors, respectively.

The fact that the viscous exponent n and the reference strain rate $\dot{\gamma}_0$ are the same for all the slip systems and grains in a given polycrystal simplifies the analysis considerably. The local potential u is in this case a homogeneous function of degree $n+1$ in $\boldsymbol{\sigma}$, and consequently, the corresponding effective potential $\widetilde{u}$ is a homogeneous function of degree $n+1$ in $\overline{\boldsymbol{\sigma}}$ (Ponte

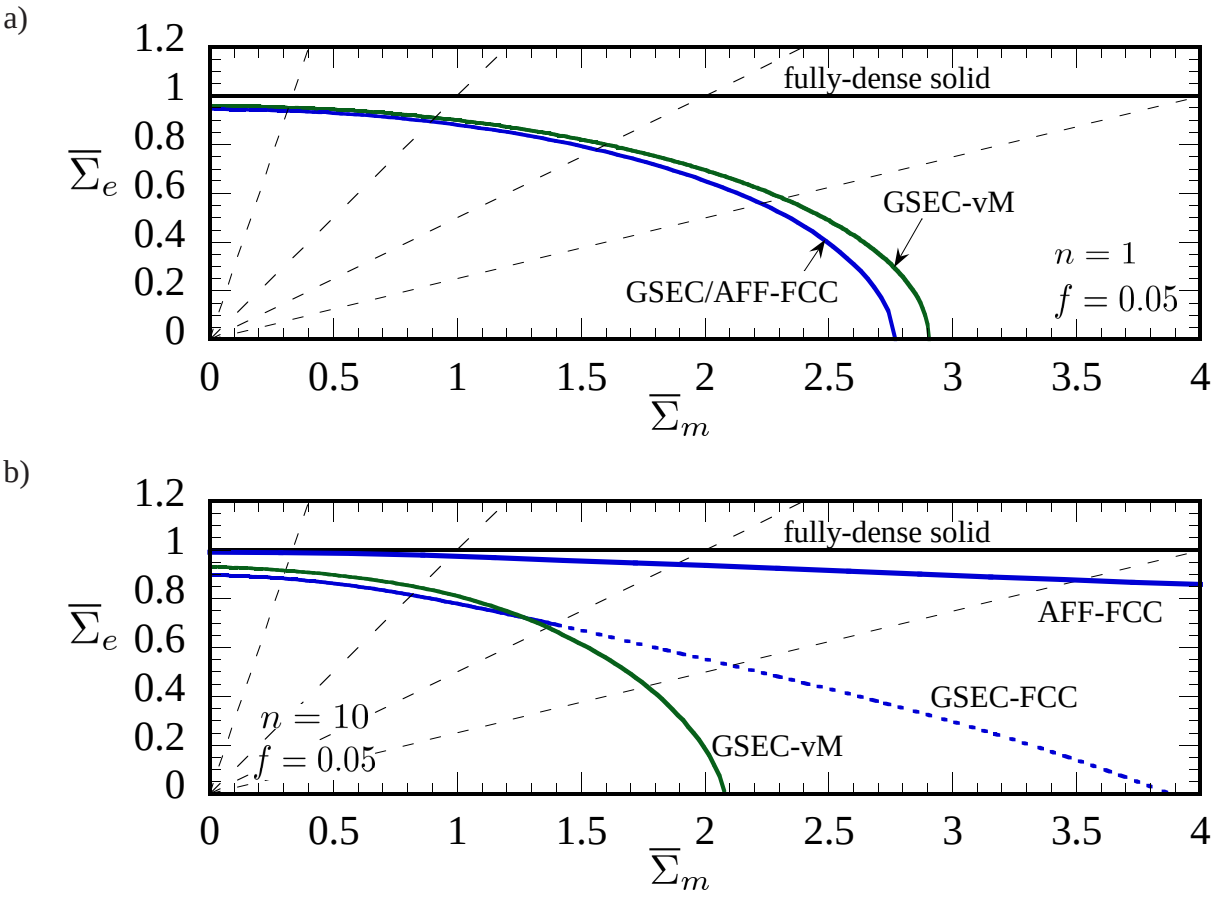

Figure 2: 'Generalized-secant' (GSEC) estimates for the gauge surfaces of untextured fcc polycrystalline solids with porosity level $f = 0.05$ and viscous exponents (a) $n = 1$ and (b) $n = 10$. Dashed lines indicate directions of constant stress triaxialities $\overline{X}_\sigma = 1/3, 1, 2, 4$.

Castañeda and Suquet, 1998). Then, a single equipotential surface $\widetilde{u}(\overline{\boldsymbol{\sigma}})$ =constant in $\overline{\boldsymbol{\sigma}}$-space fully characterizes $\widetilde{u}$; any other equipotential surface is simply a homothetic surface (Leblond et al., 1994). Results for power-law polycrystals are reported here in the form of equipotential surfaces given by

$$\left\{ \overline{\boldsymbol{\Sigma}} : \ \widetilde{u}(\overline{\boldsymbol{\Sigma}}) = \frac{\sigma_0^{-n}\dot{\gamma}_0}{n+1} \right\}, \tag{14}$$

where σ_0 is some reference flow stress —see below. This is the so-called *gauge surface* of the polycrystal, which characterizes completely the effective response (Leblond et al., 1994). The 'normal' to this surface in $\overline{\boldsymbol{\sigma}}$-space dictates the direction of macroscopic plastic flow in $\overline{\boldsymbol{D}}$-space. In the ideally-plastic limit, the gauge surface reduces to the yield surface of the aggregate. With the objective of comparing predictions for polycrystalline and isotropic von Mises solids, we will report gauge surfaces for *voided* polycrystals with σ_0 being the flow stress of the corresponding *fully dense* polycrystal with *isotropic* crystallographic and morphological textures. The values are taken from the work of Lebensohn et al. (2010): $\sigma_0 = 1.499\tau_0$ for $n = 1$ and $\sigma_0 = 2.574\tau_0$ for $n = 10$. Finally, we recall for later use that the overall stress triaxiality $\overline{X}_\sigma$ is defined as the ratio of the hydrostatic stress $\overline{\sigma}_m$ to the von Mises equivalent stress $\overline{\sigma}_e$, and that uniaxial tension corresponds to $\overline{X}_\sigma = 1/3$. Corresponding invariants of $\overline{\boldsymbol{\Sigma}}$ in (14) are defined similarly.

The simultaneous effect of crystallinity and porosity on the effective response is explored in fig. 2. The generalized-secant (GSEC) predictions for fcc polycrystals correspond to two hundred ($N = 200$) equi-weighted grain orientations prescribed according to some random process in order to generate solids with a fairly isotropic effective response. For reasons that will become evident shortly, generalized-secant (GSEC) surfaces for $n = 10$ have been plotted in continuous lines for $\overline{X}_\sigma \leq 2$ but in dotted lines for $\overline{X}_\sigma > 2$. The effect of crystallinity is assessed by comparing polycrystal estimates with GSEC estimates for von Mises voided solids derived by Danas et al. (2008). Also shown in this figure for comparison purposes are the 'affine' (AFF) estimates proposed by Masson et al. (2000). These 'classical' linear-comparison estimates of the self-consistent type make use of a linearization scheme based on the first moments of the fields only. In the representation of fig. 2, the gauge surface of a fully dense solid with either polycrystalline or von Mises matrix is given by the line $\overline{\Sigma}_e = 1$, parallel to the hydrostatic axis. We begin by noting that for $n = 1$ the GSEC and AFF estimates agree exactly with the underlying self-consistent estimates on which they are based, but for $n = 10$ they give diverging predictions. The GSEC surface for $n = 10$ is closed and convex, as it should, while the AFF surface is non-convex and exhibits an unbounded hydrostatic strength. The poor performance of classical models like the affine model at large triaxialities is a direct consequence of a linearization scheme solely based on the first moments of the local fields. The generalized-secant linearization scheme, on the other hand, involves the second moments and as a consequence gives superior predictions. At low to moderate triaxialities ($0 \leq \overline{X}_\sigma \lesssim 2$) GSEC estimates predict an increasing weakening effect —due to the presence of voids— with increasing nonlinearity n, but a minor influence of matrix crystallinity within the entire range of nonlinearities considered. At large triaxialities, on the other hand, opposite trends are observed: for $n = 10$, the predicted hydrostatic strength of the voided polycrystal is almost two times that of the von Mises solid. However, as discussed in more detail below, generalized-secant predictions at large triaxialities should be taken with caution.

We now assess the effect of crystallographic texture and porosity on the effective response. A sharp rolling texture is simulated by a set of one thousand ($N = 1000$) crystal orientations. The anisotropic specimens are loaded in axisymmetric tension along three mutually orthogonal directions: the rolling, normal and transverse directions. Also included in these figures for comparison purposes are the corresponding gauge surfaces for von Mises voided solids. Once again, we note that GSEC surfaces are closed and convex, as expected, and exhibit the same trends with increasing nonlinearity as those observed previously for untextured polycrystals. The main observation, however, is that GSEC estimates predict a minor influence of crystallographic texture on the effective response of fcc polycrystals, and particularly so at the hydrostatic point.

Now, while very accurate at low to moderate triaxialities, $0 \leq \overline{X}_\sigma \lesssim 2$, linear-comparison estimates like GSEC estimates are known to give overly strong predictions at larger triaxialities. In fact, they are found here to exhibit a corner at the hydrostatic point while smoothness is expected. As a result, GSEC predictions for highly triaxial creeping processes will give unrealistically small hydrostatic strain rates and consequently, will underestimate void growth at the initial stages of deformation. This problem of variational linear-comparison estimates is already well known in the context of von Mises voided solids (see, for instance, Pastor and Ponte Castañeda, 2002; Bilger et al., 2002). In this connection, Danas et al. (2008) have proposed an ad-hoc remedy whereby the linearization scheme is forced to depend explicitly on the macroscopic stress triaxiality in such a way that the effective gauge surface tends to some specified hydrostatic point. In the case of von Mises solids, a suitable hydrostatic point is available from the well-known solution of a hollow shell. A similar strategy could be envisaged for voided

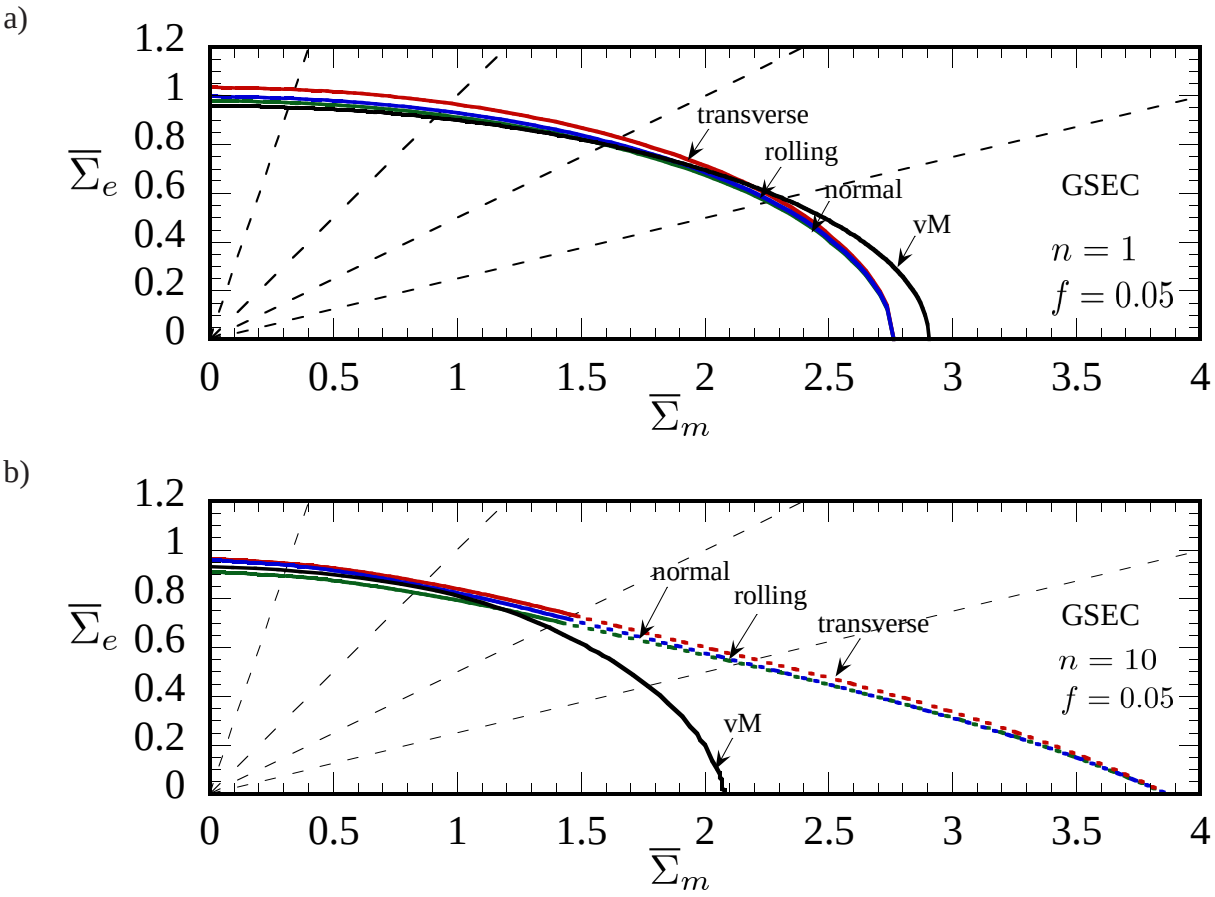

Figure 3: 'Generalized-secant' (GSEC) estimates for the gauge surfaces of textured fcc polycrystalline solids with porosity level $f = 0.05$ and viscous exponents (a) $n = 1$ and (b) $n = 10$. Dashed lines indicate directions of constant stress triaxialities $\overline{X}_\sigma = 1/3, 1, 2, 4$.

polycrystalline solids and will be explored in future work; in this connection, the recent work of Idiart (2007, 2008) for sequentially laminated composites could prove helpful. In any event, as it stands, the generalized-secant theory proposed in this work should be accurate enough to model deformation processes involving low to moderate stress triaxialities.

Thus, this study shows that, at least at low to moderate stress triaxialities, the usual assumption of matrix isotropy made in most available theories of dilatational viscoplasticity —such as Gurson's theory (Gruson, 1977) and its generalizations (e.g., Leblond et al., 1994)— should be reasonable for cubic polycrystals, even for specimens exhibiting strong crystallographic textures. Of course, this is so provided other sources of anisotropy such as morphological texture and anisotropic distributions of second-phase particles are absent.

Acknowledgements

The work of RAL was supported by Joint DoD/DOE Munitions Technology Program and LANL LDRD-DR 2010026 Programs. The work of PPC was partially supported by Joint DoD/DOE Munitions Technology Program under LANL subcontract number 76847-001-09.

REFERENCES

[1] Bache M.R., Evans W.J. Impact of texture on mechanical properties in an advanced titanium alloy. *Mater. Sci. Eng. A* 319–321:409–414, 2001.

[2] Bilger N., Auslender F., Bornert M., Masson R. New bounds and estimates for porous media with rigid perfectly plastic matrix. *C. R. Mécanique* 330:127-, 2002.

[3] Danas K., Idiart M.I., Ponte Castañeda P. A homogenization-based constitutive model for isotropic viscoplastic porous media. *Int. J. Solids Struct.* 45:3392–3409, 2008.

[4] Gray III G.T., Bourne N.K., Zocher M.A., Maudlin P.J., Millett J.C.F. Influence of crystallographic anisotropy on the Hopkinson fracture "spallation" of zirconium. In M.D. Furnish, L.C. Chhabildas and R.S. Hixson, editors, *Shock Compression of Condensed Matter - 1999*, Woodbury (NY), U.S.A., pp. 509–512, 2000.

[5] Groves G.W., Kelly A. Independent slip systems in crystals. *Phil. Mag.* 8:877–887, 1953.

[6] Gurson A.L. Continuum theory of ductile rupture by void nucleation and growth: Part I – Yield criteria and flow rules for porous ductile media. *J. Engng. Mat. Tech.* 99:2–15, 1977.

[7] Hales S.J., Hafley R.A. Texture and anisotropy in Al-Li alloy 2195 plate and near-net-shape extrusions. *Mater. Sci. Eng. A* 257:153–164, 1998.

[8] Idiart M.I. Nonlinear sequential laminates reproducing hollow sphere assemblages. *C. R. Mecanique* 335:363–368, 2007.

[9] Idiart M.I. Modeling the macroscopic behavior of two-phase nonlinear composites by infinite-rank laminates. *J. Mech. Phys. Solids* 56:2599–2617, 2008.

[10] Lebensohn, R.A., Tomé C.N., Maudlin P.J. A selfconsistent formulation for the prediction of the anisotropic behavior of viscoplastic polycrystals with voids. *J. Mech. Phys. Solids* 52:249–278, 2004.

[11] Lebensohn R.A., Liu Y., Ponte Castañeda P. On the accuracy of the self-consistent approximation for polycrystals: comparison with full-field numerical simulations. *Acta Mater.* 52:5347–5361, 2004.

[12] Lebensohn R.A., Tomé C.N., Maudlin P.J. Modelling the anisotropic behavior of polycrystals with voids. In: S.R. Idelsohn, V.E. Sonzogni and A. Cardona, editors, Mecánica Computacional Vol. XXI, Santa Fe-Paraná, Argentina, pp. 1075–1082, 2002.

[13] Lebensohn R.A., Solas D., Canova G., Brechet Y. Modelling damage of Al-Zn-Mg alloys. *Acta Mater.* 44:315–325, 1996.

[14] Lebensohn R.A., Idiart M.I., Ponte Castañeda P., Vincent P.-G. Dilatational viscoplasticity of polycrystalline solids with intergranular cavities. In preparation.

[15] Leblond J.B., Perrin G., Suquet P. Exact results and approximate models for porous viscoplastic solids. *Int. J. Plasticity* 10:213–235, 1994.

[16] Liu Y., Ponte Castañeda P. Second-order theory for the effective behavior and field fluctuations in viscoplastic polycrystals. *J. Mech. Phys. Solids* 52:467–495, 2004.

[17] Masson R., Bornert M., Suquet P., Zaoui A. An affine formulation for the prediction of the effective properties of nonlinear composites and polycrystals. *J. Mech. Phys. Solids* 48:1203–1227, 2000.

[18] Ponte Castañeda P., Suquet P. Nonlinear composites. *Adv. Appl. Mech.* 34:171–302, 1998.

[19] Tomé C.N., Lebensohn R.A., Manual for code viscoplastic self-consistent (version 7). Available at: http://public.lanl.gov/lebenso/vpscmanual.pdf

[20] Willis J.R. Bounds and self-consistent estimates for the overall moduli of anisotropic composites. *J. Mech. Phys. Solids* 25:185–202, 1977.

[21] Willis J.R. Variational and related methods for the overall properties of composites. *Adv.*

Appl. Mech. 21:1–78, 1981.